Assessment of the models for predicting the responses of spherical objects in viscoelastic mediums and at viscoelastic interfaces

H Koruk[1]

[1]Mechanical Engineering Department, MEF University, 34396 Istanbul, Turkey

E-mail: korukh@mef.edu.tr

Abstract. Spherical objects, such as bubbles and spheres, embedded in mediums and at viscoelastic interfaces are encountered in many applications, including the determination of material properties. This paper assesses the models for predicting the responses of spherical objects in viscoelastic mediums and at viscoelastic interfaces used in various applications. The models are presented very compactly, and evaluations are performed based on the analyses of the models for the spherical objects in viscoelastic mediums and at viscoelastic interfaces. First, the models for predicting the static displacements of spherical objects are presented and assessed. After that, the models for predicting the dynamic responses of spherical objects are presented and their dynamic behaviours are compared. Then, the models for the deformation of the medium around spherical objects and stress distribution are presented and evaluated. The models and evaluations presented in this study can be exploited in various applications, including biomedical applications.

1. Introduction

Spherical objects, such as bubbles and spheres, embedded in mediums and at viscoelastic interfaces are encountered in many applications [1-4]. For example, bubbles and spheres embedded in a medium have been used to determine material properties, such as the Young's modulus [1,5]. Microbubbles at interfaces are used in therapeutic and diagnostic ultrasound applications [6,7]. Similarly, spheres at interfaces are exploited in atomic force microscopy or indentation tests [8-10]. There have been many studies in recent years to understand the responses of spherical objects in mediums and at viscoelastic interfaces, and to reveal their applications [5,7,11-17]. However, the models for predicting the responses of spherical objects in viscoelastic mediums and at viscoelastic interfaces have not been compared and evaluated in the literature so far.

The models for predicting the responses of bubbles and spheres in viscoelastic mediums and at viscoelastic interfaces are presented and evaluated in this paper. Here, the models are presented very compactly, and evaluations are performed based on the analyses of the models for the spherical objects in viscoelastic mediums and at viscoelastic interfaces. The spherical object with a radius R embedded in a viscoelastic medium and at a viscoelastic interface with a shear modulus G, density ρ and viscosity η is illustrated in Figure 1. Here, first, the models for predicting the static displacements of

spherical objects are presented and assessed. After that, the models for predicting the dynamic responses of spherical objects are presented and their dynamic behaviours are compared. Then, the models for predicting the deformation of the medium around the spherical objects and stress distribution are presented and evaluated.

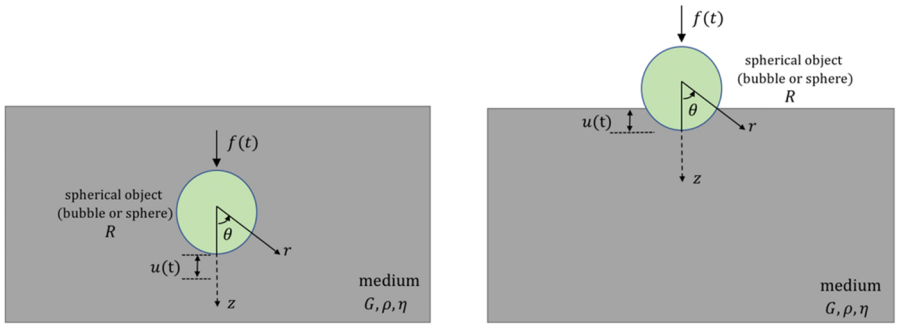

Figure 1. The spherical object embedded in a viscoelastic medium (left) and at a viscoelastic interface (right).

2. Static displacements of the spherical objects

(1) The displacement of the bubble embedded in a soft medium for a static force is given by [11]:

$$u = \frac{f_0}{4\pi GR} \tag{1}$$

(2) The displacement of the bubble at a soft interface for a static force is defined by [14]:

$$u = \frac{f_0}{2\pi GR\left[1-\left(1-\frac{u}{R}\right)^3\right]} \tag{2}$$

(3) The displacement of the sphere embedded in a soft medium for a static force is given by [11]:

$$u = \frac{f_0}{6\pi GR} \tag{3}$$

(4) The displacement of the sphere at an interface for a static force is given by [18]:

$$u = \left(\frac{3f_0}{4E^*\sqrt{R}}\right)^{2/3} \tag{4}$$

Here, f_0 is the force amplitude, G is the shear modulus of the medium, E^* is the reduced Young's modulus, computed as $1/E^* = \left(1-\nu_{\text{sphere}}^2\right)/E_{\text{sphere}} + (1-\nu^2)/E$ and R is the radius of the spherical object. E and ν are the Young's modulus and Poisson's ratio of the medium, respectively. For a rigid sphere, the reduced Young's modulus becomes $E^* = E/(1-\nu^2)$. The elasticity modulus is related to the shear modulus by $E = 2G(1+\nu)$ for homogeneous isotropic materials.

The stiffness for the four models presented above is plotted as a function of the displacement of the spherical objects in Figure 2. Here, the stiffness is normalized by GR (i.e., $\frac{f_0}{uGR}$) and the displacement is normalized by R (i.e., $\frac{u}{R}$). It is seen that the stiffness of the bubble and sphere embedded in the medium are constant. On the other hand, the stiffness changes nonlinearly with the displacement for the spherical objects at interfaces. The stiffness of the sphere in the medium, the bubble in the medium, and the bubble at the interface is approximately 4.2, 2.8, and 1.4 times, respectively, greater than the stiffness of the sphere at the interface for a displacement equal to the radius of the spherical objects (i.e., $u = R$).

The normalized force (i.e., $\frac{f_0}{GR}$) required for a specific normalized displacement for the four systems presented above is plotted in Figure 3. It is seen that the force required for a specific displacement is highest for the sphere embedded in the medium and lowest for the sphere at the interface. The force required for a specific displacement for the bubble embedded in the medium is higher than the one for the bubble at the interface.

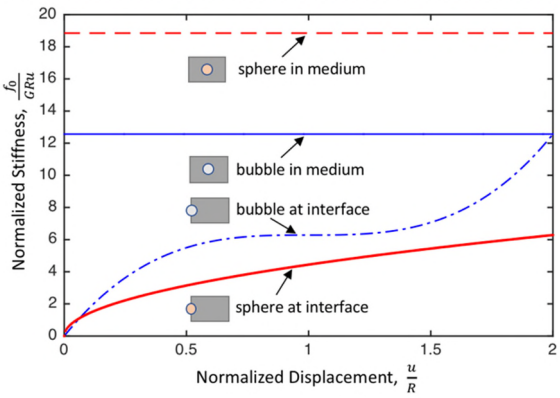

Figure 2. The normalized stiffness as a function of normalized displacement.

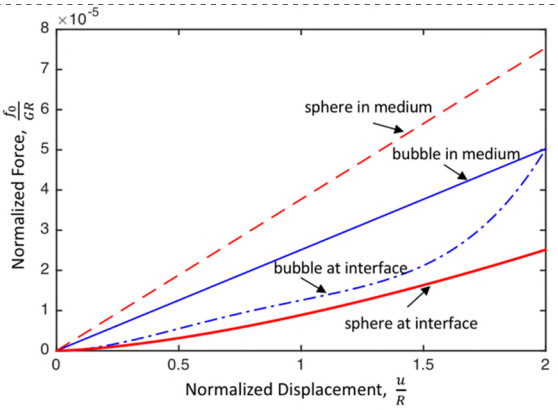

Figure 3. The normalized force as a function of normalized displacement.

3. Dynamic responses of the spherical objects

(i) The frequency-domain equation that couples the displacement of the bubble embedded in a soft viscoelastic medium for a dynamic force is [11]:

$$4\pi(G-j\omega\eta)RU\left(1-jkR-\frac{1}{6}k^2R^2+\frac{1}{18}jk^3R^3\right)=F \tag{5}$$

where $k=\frac{\omega}{\sqrt{(G-j\omega\eta)/\rho}}$ is the complex wave number of the shear wave with the frequency ω, ρ and η are the density and viscosity of the medium, $j=\sqrt{-1}$, F is the Fourier transform of the external force $f(t)$, and U is a spectral component of the bubble displacement. Let's now consider the external force as a rectangular pulse with an amplitude of f_0 and a duration of τ (i.e., the constant force f_0 is applied for a short time τ and then removed). It should be remembered that the response to the rectangular pulse simulates the impulse response for small τ values and the step response for large τ values with $0\le t\le\tau$. It can be calculated that the Fourier transform of the rectangular pulse is $F=-\frac{jf_0}{\omega}\left(e^{j\omega\tau}-1\right)$. Hence, the dynamic displacement of the bubble in the viscoelastic medium can be determined using:

$$u(t)=-\frac{jf_0}{24\pi^2R}\int_{-\infty}^{\infty}\frac{\left(e^{j\omega\tau}-1\right)(3-jkR)e^{-j\omega t}}{\omega(G-j\omega\eta)\left(1-jkR-\frac{1}{6}k^2R^2+\frac{1}{18}jk^3R^3\right)}\mathrm{d}\omega \tag{6}$$

(ii) The frequency-domain equation that couples the displacement of the bubble at a soft viscoelastic medium interface for a dynamic force is given by [14,15]:

$$2\pi(G-j\omega\eta)RU(1-cos^3\theta_u)\left(1-jkR-\frac{1}{6}k^2R^2+\frac{1}{18}jk^3R^3\right)=F \tag{7}$$

where θ_u is the angle corresponding to the displacement $u(t)$. The dynamic displacement of the bubble at the viscoelastic medium interface can be determined using:

$$u(t)=-\frac{jf_0}{12\pi^2R\left\{1-\left[1-\frac{u(t)}{R}\right]^3\right\}}\int_{-\infty}^{\infty}\frac{\left(e^{j\omega\tau}-1\right)(3-jkR)e^{-j\omega t}}{\omega(G-j\omega\eta)\left(1-jkR-\frac{1}{6}k^2R^2+\frac{1}{18}jk^3R^3\right)}\mathrm{d}\omega \tag{8}$$

(iii) The frequency-domain equation that couples the displacement of the sphere embedded in a soft viscoelastic medium for a dynamic force is given as [12]:

$$-m_s\omega^2 U + 6\pi(G - j\omega\eta)RU\left(1 - jkR - \frac{1}{9}k^2R^2\right) = F \tag{9}$$

Here $m_s = \frac{4}{3}\pi R^3\rho_s$ is the mass of the sphere where ρ_s is the density of the sphere. The dynamic displacement of the sphere in the viscoelastic medium can be determined using:

$$u(t) = -\frac{jf_0}{12\pi^2 R}\int_{-\infty}^{\infty}\frac{(e^{j\omega\tau}-1)e^{-j\omega t}}{\omega\left[-\frac{2}{9}R^2\rho_s\omega^2+(G-j\omega\eta)\left(1-jkR-\frac{1}{9}k^2R^2\right)\right]}\mathrm{d}\omega \tag{10}$$

(iv) The frequency-domain equation that couples the displacement of the sphere at a viscoelastic medium interface for a dynamic force can be expressed as follows [17]:

$$-\frac{2}{9}\pi R^3(4\rho_s+\rho)\omega^2 U + f_0^{1/3}\left[\frac{8(G-j\omega\eta)(1+\nu)\sqrt{R}}{3(1-\nu^2)}\right]^{2/3}\left(1-\frac{1}{2}j\omega\sqrt{\frac{\rho}{G-j\omega\eta}}R\right)U = F \tag{11}$$

The dynamic displacement of the sphere at the viscoelastic medium interface can be determined using:

$$u(t) = \frac{1}{2\pi}\int_{-\infty}^{\infty}\frac{(-jf_0/\omega)(e^{j\omega\tau}-1)}{-\frac{2}{9}\pi R^3(4\rho_s+\rho)\omega^2+f_0^{1/3}\left[\frac{8(G-j\omega\eta)(1+\nu)\sqrt{R}}{3(1-\nu^2)}\right]^{2/3}\left(1-\frac{1}{2}j\omega\sqrt{\frac{\rho}{G-j\omega\eta}}R\right)}\mathrm{d}\omega \tag{12}$$

The dynamic responses of spherical objects with a radius of R = 2 μm in a viscoelastic medium and at a viscoelastic interface (G = 2000 Pa, ρ = 1000 kg/m^3, η = 0.2 Pa s, ν = 0.45) for a force of f_0 = 0.015 μN and two different durations are plotted in Figure 4. Here, the time duration is divided into N points (e.g., 500), and the calculations are repeated over the entire period of interest using Matlab (MathWorks, Natick, MA, USA) to find the dynamic responses of spherical objects. It is seen that the rate of relaxation is lowest for the bubble at the interface. A force of f_0 = 0.015 μN (or 15 nN) produces a steady-state displacement of approximately 0.20, 0.28, 0.78, and 1.13 μm for the sphere in the medium, the bubble in the medium, the bubble at the interface, and the sphere at the interface, respectively, for a radius of R = 2 μm.

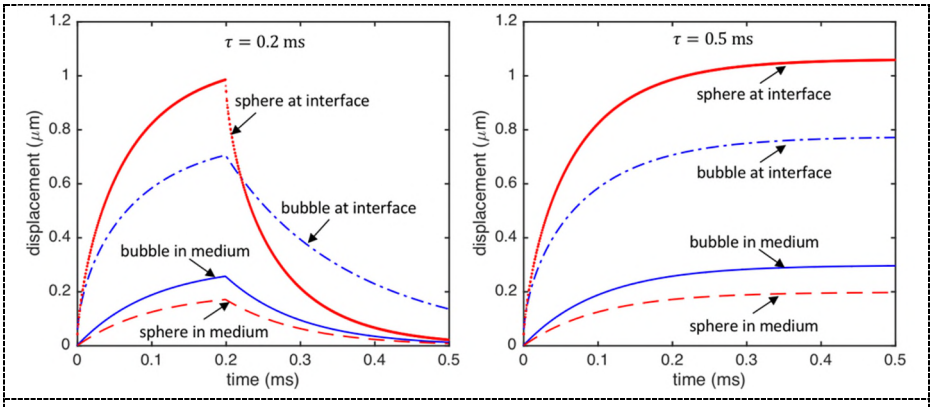

Figure 4. Displacements of spherical objects (G = 2000 Pa, ρ = 1000 kg/m^3, η = 0.2 Pa s, ν = 0.45, R = 2 μm, ρ_s = 3000 kg/m^3, f_0 = 0.015 μN).

The dynamic responses of spherical objects with a radius of R = 100 μm in a viscoelastic medium and at a viscoelastic interface (G = 2000 Pa, ρ = 1000 kg/m^3, ν = 0.45) with two different viscosity values and a force of f_0 = 30 μN are plotted in Figure 5. It is seen that, for all the four cases, only the sphere at the interface oscillates (when η = 0.2 Pa s). However, the sphere does not have any oscillations when the viscosity is increased (η = 0.5 Pa s). It is seen that the viscosity does not change the steady-

state displacements of the spherical objects. The results show that the force producing a displacement of $u = R$ is tens of nano-Newton for spherical objects with a diameter of a few micro meters. The corresponding force is tens of micro-Newton for spherical objects with a diameter of hundred micro meters.

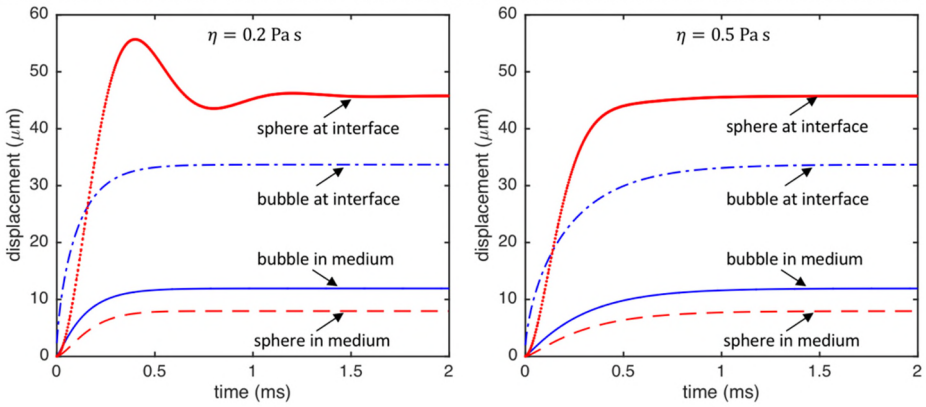

Figure 5. Displacements of spherical objects (G = 2000 Pa, ρ = 1000 kg/m3, v = 0.45, R = 100 μm, ρ_s = 3000 kg/m^3, f_0 = 30 μN).

4. Deformation of the medium around spherical objects and stress distribution

(a) Using the formulations by Ilinskii et al. [11], the deformation of the medium and the nonzero stress component for the bubble embedded in a soft medium can be written as:

$$u_r(r,\theta,t) = \frac{R}{r}u(t)\cos(\theta) \tag{13a}$$

$$u_\theta(r,\theta,t) = -\frac{R}{2r}u(t)\sin(\theta) \tag{13b}$$

$$\sigma_r(r,\theta,t) = -\frac{2GR}{r^2}u(t)\cos(\theta) \tag{14}$$

where $u(t)$ is given by equations (1) and (6) for static and dynamic loading, respectively. (b) Using the formulations by Koruk and Choi [14], the deformation of the medium and the nonzero stress component for the bubble at a soft interface can be written as:

$$u_r(r,\theta,t) = \frac{R}{r}u(t)\cos(\theta) \tag{15a}$$

$$u_\theta(r,\theta,t) = -\frac{R}{2r}u(t)\sin(\theta) \tag{15b}$$

$$\sigma_r(r,\theta,t) = -\frac{2GR}{r^2}u(t)\cos(\theta) \tag{16}$$

where $u(t)$ is given by equations (2) and (8) for static and dynamic loading, respectively. (c) Using the formulations by Ilinskii et al. [11], the deformation of the medium and the nonzero stress component for the sphere embedded in a soft medium can be written as:

$$u_r(r,\theta,t) = u(t)\left(\frac{3R}{2r} - \frac{R^3}{2r^3}\right)\cos(\theta) \tag{17a}$$

$$u_\theta(r,\theta,t) = -u(t)\left(\frac{3R}{4r} + \frac{R^3}{4r^3}\right)\sin(\theta) \tag{17b}$$

$$\sigma_r(r,\theta,t) = -\frac{3G}{r}u(t)\left(\frac{R}{r} - \frac{R^3}{r^3}\right)\cos(\theta) \tag{18a}$$

$$\sigma_\theta(r,\theta,t) = \frac{3G}{2r^4}u(t)R^3\sin(\theta) \tag{18b}$$

where $u(t)$ is given by equations (3) and (10) for static and dynamic loading, respectively. (d) The radius of the contact area caused by the sphere at an interface and the maximum pressure within the contact area can be written as:

$$a = \sqrt{Ru(t)} \tag{19}$$

$$p_{\max} = \frac{3f_0}{2\pi Ru(t)} \tag{20}$$

where $u(t)$ is given by equations (4) and (12) for static and dynamic loading, respectively. The stresses underneath the contact area are:

$$\sigma_x = \sigma_y = -p_{\max}\left\{\left[1 - \left|\frac{z}{a}\right| \operatorname{atan}\frac{1}{|z/a|}\right](1+v) - \frac{1}{2(1+z^2/a^2)}\right\} \tag{21a}$$

$$\sigma_z = -\frac{p_{\max}}{1+z^2/a^2} \tag{21b}$$

The stress developed in the viscoelastic medium (G = 2000 Pa, ρ = 1000 kg/m^3, v = 0.45) underneath the spherical object with a radius of R = 2 μm as a function of position for a force of f_0 = 0.015 μN is plotted in Figure 6. Here, the position is measured from the tip contact point and normalized by the radius (i.e., $\frac{p}{R}$). It is seen that the stress is maximum at the tip contact point (p = 0) for the bubble while it is maximum at p/R = 0.4 for the sphere. For the same force level, the magnitude of the maximum stress is approximately 150, 600, 1550, and 1850 Pa for the sphere in the medium, the bubble in the medium, the bubble at the interface, and the sphere in the interface, respectively. As expected, the stress approaches zero far from the contact point for all cases (being negligible for p/R > 8).

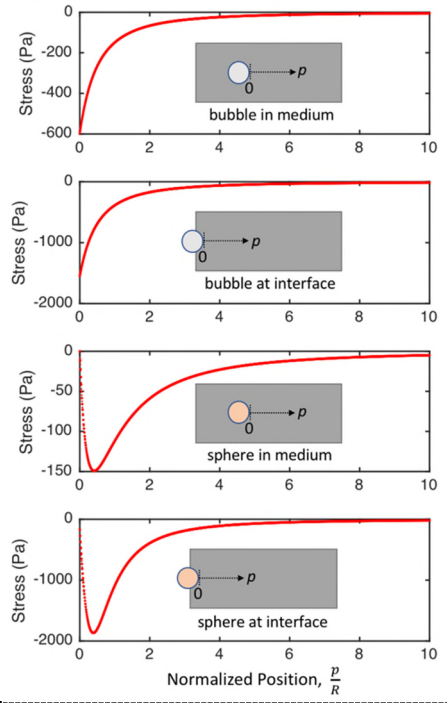

Figure 6. Stress distribution underneath the tip contact point (G = 2000 Pa, ρ = 1000 kg/m^3, v = 0.45, R = 2 μm, f_0 = 0.015 μN).

5. Concluding remarks

In this paper, the models for predicting the responses of spherical objects in viscoelastic mediums and at viscoelastic interfaces are assessed. First, the models for predicting the static displacements of

spherical objects are presented and assessed. After that, the models for predicting the dynamic responses of spherical objects are presented and their dynamic behaviors are compared. Then, the models for predicting the deformation of the medium around the spherical objects and stress distribution are presented and evaluated.

- The force increases linearly with the displacement of the bubble and sphere embedded in a medium, though it changes nonlinearly with the displacement of the bubble and sphere at an interface. The force needed for a displacement equal to the radius of the spherical object for the sphere in the medium, the bubble in the medium, and the bubble at the interface is approximately 4.2, 2.8, and 1.4 times, respectively, greater than that of the sphere at the interface. The force producing a steady-state displacement equal to the radius of the spherical object is tens of nano-Newton for spherical objects with a diameter of a few micro meters (for a medium shear modulus of a few thousand Pascal). The corresponding force is tens of micro-Newton for spherical objects with a diameter of hundred micro meters.
- The rate of relaxation is low for the bubble at the interface, compared to the sphere at the interface and the bubble and sphere in the medium. For the same radius and material properties, although there are no oscillations for all other three systems, the sphere at the interface can oscillate. However, the sphere does not have any oscillations when its radius is small and the medium viscosity is high. The viscosity does not change the steady-state displacements of the spherical objects.
- The stress is maximum at the tip contact point for the bubble, while it is maximum at the point where the ratio of position to radius is 0.4 for the sphere. For the same level of force, the magnitude of the maximum stress for the bubble in the medium, the bubble at the interface, and the sphere in the interface is approximately 4, 10, and 12 times, respectively, greater than that for the sphere in the medium. For all four cases, stress is negligible when the ratio of position to radius is greater than 8.

The models and evaluations presented in this study can be used in many practical applications. For example, they can be used to design experiments and to identify the elastic and damping properties of materials at the nano- and micro-scale in biomedical applications. They can be exploited to determine the responses of spherical objects in viscoelastic mediums and at viscoelastic interfaces, and to identify the stresses developed in mediums around the spherical objects in practical applications. The experimental evaluation of the four cases presented in this paper is considered as the topic of a future work.

References

[1] Chen S, Fatemi M and Greenleaf J F. Remote measurement of material properties from radiation force induced vibration of an embedded sphere. *The Journal of the Acoustical Society of America*, 884–889, 112 (3), 2002.

[2] Rigaud E and Perret-Liaudet J. Experiments and numerical results on non-linear vibrations of an impacting Hertzian contact. Part 1: harmonic excitation. *Journal of Sound and Vibration*, 289-307, 265 (2), 2003.

[3] Cheng L, Xia X, Scriven L E and Gerberich W W. Spherical-tip indentation of viscoelastic material. *Mechanics of Materials,* 213–226, 37 (1), 2005.

[4] Karpiouk A B, Aglyamov S R, Ilinskii Y A, Zabolotskaya E A and Emelianov S Y. Assessment of shear modulus of tissue using ultrasound radiation force acting on a spherical acoustic inhomogeneity. *IEEE Transactions on Ultrasonics, Ferroelectrics, and Frequency Control*, 2380–2387, 56 (11), 2009.

[5] Erpelding T N, Hollman K W and O'Donnell M. Bubble-based acoustic radiation force elasticity imaging. *IEEE Transactions on Ultrasonics, Ferroelectrics, and Frequency Control*, 971–979, 52 (6), 2005.

[6] Acconcia C, Leung B Y C, Hynynen K and Goertz D E. Interactions between ultrasound stimulated microbubbles and fibrin clots. *Applied Physics Letters,* 53701, 103 (5), 2013.
[7] Pouliopoulos A N, Burgess M T and Konofagou E E. Pulse inversion enhances the passive mapping of microbubble-based ultrasound therapy. *Applied Physics Letters,* 44102, 113, 2018.
[8] Garcia R and San Paulo A. Dynamics of a vibrating tip near or in intermittent contact with a surface. *Physical Review B*, R13381-R13384, 61 (20), 2000.
[9] Dimitriadis E K, Horkay F, Maresca J, Kachar B and Chadwick R S. Determination of elastic moduli of thin layers of soft material using the atomic force microscope. *Biophysical Journal,* 2798–2810, 82 (5), 2002.
[10] Tan E P S and Lim C T. Nanoindentation study of nanofibers. *Applied Physics Letters,* 123106, 87 (12), 2005.
[11] Ilinskii Y A, Meegan G D, Zabolotskaya E A and Emelianov S Y. Gas bubble and solid sphere motion in elastic media in response to acoustic radiation force. *The Journal of the Acoustical Society of America*, 2338–2346, 117 (4), 2005.
[12] Aglyamov S R, Karpiouk A B, Ilinskii Y A, Zabolotskaya E A and Emelianov S Y. Motion of a solid sphere in a viscoelastic medium in response to applied acoustic radiation force: Theoretical analysis and experimental verification. *The Journal of the Acoustical Society of America*, 1927-1936, 122 (4), 2007.
[13] Koruk H, El Ghamrawy A, Pouliopoulos A N and Choi J J. Acoustic particle palpation for measuring tissue elasticity. *Applied Physics Letters,* 223701, 107 (22), 2015.
[14] Koruk H and Choi J J. Displacement of a bubble by acoustic radiation force into a fluid–tissue interface. *The Journal of the Acoustical Society of America*, 2535–2540, 143 (4), 2018.
[15] Koruk H and Choi, J J. Displacement of a bubble located at a fluid-viscoelastic medium interface. *The Journal of the Acoustical Society of America*, EL410–EL416, 145 (5), 2019.
[16] Bezer J H, Koruk H, Rowlands C J and Choi J J. Elastic deformation of soft tissue-mimicking materials using a single microbubble and acoustic radiation force. *Ultrasound in Medicine & Biology*, 3327-3338, 46 (12), 2020.
[17] Koruk H. Development of a model for predicting dynamic response of a sphere at viscoelastic interface: A dynamic Hertz model. *IOP Conference Series: Materials Science and Engineering*, 2021.
[18] Johnson K L. *Contact Mechanics* (Cambridge University Press), 1985.